


RESEARCH

Open Access



Differential expression of receptors mediating receptor-mediated transcytosis (RMT) in brain microvessels, brain parenchyma and peripheral tissues of the mouse and the human

Wandong Zhang^{1*} , Qing Yan Liu¹, Arsalan S. Haqqani¹, Sonia Leclerc¹, Ziyang Liu², François Fauteux², Ewa Baumann¹, Christie E. Delaney¹, Dao Ly¹, Alexandra T. Star¹, Eric Brunette¹, Caroline Sodja¹, Melissa Hewitt¹, Jagdeep K. Sandhu¹ and Danica B. Stanimirovic^{1*}

Abstract

Receptor-mediated transcytosis (RMT) is a principal pathway for transport of macromolecules essential for brain function across the blood–brain barrier (BBB). Antibodies or peptide ligands which bind RMT receptors are often co-opted for brain delivery of biotherapeutics. Constitutively recycling transferrin receptor (TfR) is a prototype receptor utilized to shuttle therapeutic cargos across the BBB. Several other BBB-expressed receptors have been shown to mediate transcytosis of antibodies or protein ligands including insulin receptor (INSR) and insulin-like growth factor-1 receptor (IGF1R), lipid transporters LRP1, LDLR, LRP8 and TMEM30A, solute carrier family transporter SLC3A2/CD98hc and leptin receptor (LEPR). In this study, we analyzed expression patterns of genes encoding RMT receptors in isolated brain microvessels, brain parenchyma and peripheral organs of the mouse and the human using RNA-seq approach. IGF1R, INSR and LRP8 were highly enriched in mouse brain microvessels compared to peripheral tissues. In human brain microvessels only INSR was enriched compared to either the brain or the lung. The expression levels of SLC2A1, LRP1, IGF1R, LRP8 and TFRC were significantly higher in the mouse compared to human brain microvessels. The protein expression of these receptors analyzed by Western blot and immunofluorescent staining of the brain microvessels correlated with their transcript abundance. This study provides a molecular transcriptomics map of key RMT receptors in mouse and human brain microvessels and peripheral tissues, important to translational studies of biodistribution, efficacy and safety of antibodies developed against these receptors.

Keywords: Blood–brain barrier, Receptor-mediated transcytosis, Isolated brain microvessels, RNAseq, Mouse and human species, IGF1R, Transferrin receptor

Background

The receptor-mediated transcytosis (RMT) is a vesicular transcellular route by which various macromolecules are transported across a barrier, typically formed by a cell monolayer [1, 2]. This process is particularly important for brain delivery of essential macromolecules, including transferrin and insulin [3–6], across the blood–brain

*Correspondence: Wandong.Zhang@nrc-cnrc.gc.ca;
Danica.Stanimirovic@nrc-cnrc.gc.ca

¹ Human Health Therapeutics Research Centre, National Research Council of Canada, 1200 Montreal Road, M54, Ottawa, ON K1A0R6, Canada
Full list of author information is available at the end of the article



© The Author(s) 2020. This article is licensed under a Creative Commons Attribution 4.0 International License, which permits use, sharing, adaptation, distribution and reproduction in any medium or format, as long as you give appropriate credit to the original author(s) and the source, provide a link to the Creative Commons licence, and indicate if changes were made. The images or other third party material in this article are included in the article's Creative Commons licence, unless indicated otherwise in a credit line to the material. If material is not included in the article's Creative Commons licence and your intended use is not permitted by statutory regulation or exceeds the permitted use, you will need to obtain permission directly from the copyright holder. To view a copy of this licence, visit <http://creativecommons.org/licenses/by/4.0/>. The Creative Commons Public Domain Dedication waiver (<http://creativecommons.org/publicdomain/zero/1.0/>) applies to the data made available in this article, unless otherwise stated in a credit line to the data.

barrier (BBB) [1, 2]. A ligand binding to a receptor on the luminal surface of brain endothelial cells (BEC) triggers ligand-receptor complex endocytosis, routing through various intracellular endosomal compartments where cargo is detached from the receptor and released on the abluminal side, while the receptor recycles 'back' to accept additional cargo molecules [7–11]. This pathway has been particularly well described for the transferrin receptor (TfR), which undergoes constitutive recycling and has been considered a 'prototypical' trigger of the RMT pathway [7–13].

Antibodies and peptide ligands against various endocytosing BBB receptors have been developed as potential molecular Trojan horses or shuttles to deliver therapeutic cargos across the BBB [2, 8–16]. Discovery strategies utilizing molecular ('omics') analyses of the BBB and screening of antibody libraries to select antibody species that can transmigrate the BBB [17–22] have yielded an experimental proof of concept for novel RMT-antibody pairs. The literature survey of BBB targets shown to mediate transcytosis of antibodies or protein ligands in various model systems *in vitro* and *in vivo*, identified the following broad classes of transporters: (a) *iron transporters*: transferrin receptor (TFRC) [3–6, 8, 12, 13]; (b) *insulin and insulin-like growth factors receptors*: INSR, IGF1R, and IGF2R [16, 23, 24]; (c) *lipid transporters*: low-density lipoprotein receptor (LDLR), LDLR-related protein 1 (LRP1), LRP8, and transmembrane protein 30A (TMEM30A/CDC50A) [25–32]; (d) *solute carrier family transporters*: glucose transporter-1 (GLUT-1)/SLC2A1 and SLC3A2/CD98hc [33, 34]; and e) *neuropeptide receptors*: leptin receptor (LEPR) [35]. Structure/function relationships, ligand interactions and signaling, and specialized biology of these receptors is vastly different (summarized briefly in Additional file 1: Table S1), expanding the spectrum of potential RMT pathways across the BBB beyond the 'canonical' mechanism of TfR recycling. Whereas the mechanisms of antibody transport by some of these targets, in particular SLC family of transporters, is not fully understood, for the purpose of this manuscript they will be considered in comparison with 'classical' RMT-triggered pathways.

The development of peptides and antibodies that bind RMT receptors as potential delivery carriers for brain-targeting biotherapeutics brought about further understanding of RMT mechanisms and underscored key limitations of various approaches. For example, evaluation of bi-specific antibodies where the TfR antibody was used as a BBB transport shuttle [36, 37] revealed TfR antibody-driven fast systemic clearance, on-target complement-mediated toxicity on TfR-rich reticulocytes, as well as species differences in transport capacity in mice and non-human primates [7, 36, 38]. Ideally, RMT

receptors targeted for the development of BBB delivery antibodies should demonstrate a high degree of BBB expression selectivity compared to peripheral organs, a high abundance in the brain endothelium, as well as low expression in the brain parenchyma [8, 9]. This profile would enable an extended systemic half-life and reduced toxicity, high efficiency of brain delivery and low target-mediated removal in the brain tissue. For translational preclinical studies, and, ultimately, for demonstration of the concept in human patients, it is also important to consider species differences in the RMT target expression [39]. Three BBB carriers targeting RMT pathway, a peptide ligand of LRP-1 (Angiopep) [26, 27, 40], anti-human INSR antibody [14, 15, 41], and anti-TfR antibody [42] are being tested in clinical trials; however, the clinical proof of concept for RMT pathway as a viable route for systemic delivery of CNS biotherapeutics remains inconclusive.

The principal objective of the current study was to compare the transcript abundance of selected receptors and transporters previously shown to mediate transport of antibodies or protein ligands into the brain in isolated brain microvessels from mouse, the principal experimental species used in pre-clinical studies, and from human, by using RNA-seq. In addition, transcript abundance for these receptors was determined in the whole brain tissue and in various peripheral organs. Significant species differences in RMT receptor abundances and distribution among brain microvessels, brain and peripheral organs were observed between mouse and human. This study suggests that the RMT target receptor abundance is an important parameter to consider in translational studies for antibody-based BBB delivery strategies.

Materials and methods

Human and mouse tissues

Samples of the human brain and lung tissues from three individuals were used in the study. Human lung tissues were from normal adjacent lung tissues of three non-small cell lung cancer (NSCLC) patients undergoing surgical resections. The surgical samples were deposited in the Lung Tumor Bank managed by the CDHA-Capital District Health Authority at Halifax, NS, Canada. All patients signed informed consent as per CDHARS/2013-271, which allowed their tissues to be archived in the CDHA Lung Tumor Bank for molecular studies. Human post mortem brain tissues (two females and one male, 73–76 years old; deceased from non-brain related pathologies) were obtained from the Human Brain and Spinal Fluid Resource Center, VAMC (Los Angeles, CA), which is sponsored by NINDS/NIMN, National Multiple Sclerosis Society, VA Greater Los Angeles Healthcare System, and Veterans Health Services and Research

Administration, Department of Veteran Affairs. The use of human tissues in this study was approved by the Research Ethics Board of the National Research Council Canada (Protocols #2013-38 and #2006-03). The use of mice in this study was approved by the Animal Care Committee of the Human Health Therapeutics Research Centre at the National Research Council of Canada (Animal User Protocol #2016-04). Mice (C57BL/6 J strain, three males, 9-month old) were perfused transcardially with heparinized saline (15 mL at 2 mL/min) and organs were collected. Brain and brain vessels were freshly isolated without freezing; other organs were frozen at -80°C until RNA isolation.

Isolation of microvessels and capillaries from tissues

Microvessels and capillaries were isolated from mouse and human brains, as well as mouse lungs using modified protocols described previously [43]. Mouse brain and lung vessels were isolated from fresh tissues, whereas all human tissues were frozen and stored at -80°C until vessel isolation. The tissues were pre-weighed and thawed briefly at room temperature. Tissue homogenization and vessel separation were performed on ice using PBS (Wisent, St-Bruno, QC) containing protease inhibitor cocktail (Sigma Aldrich, St. Louis, MO.) or using a buffer containing 150 mM NaCl, 50 mM Tris (BDH, Ward Chester, PA) pH 8.0 for mass spectrometry analysis with instruments pre-chilled on ice. Respective tissues were chopped using razor blade, placed in a 5-mL Wheaton Dounce homogenization tube (Fisher Scientific, Hampton, NH), and 5 mL of PBS buffer was added per tube. Tissue was homogenized with 10 strokes of the pestle connected to Eberbach Con-Torque Homogenizer (Fisher Scientific, Hampton, NH). The tissue homogenate was transferred onto pluriStrainers in a 50-mL conical tube with a connector ring and strainers (pluriSelect, San Diego, CA) in descending order, as follows: 300 μm , 100 μm , and 20 μm strainers and connector ring, and then gentle suction was used to filter the homogenate through strainers.

Stacked strainers were rinsed with 5–10 mL of PBS and vessels were collected by placing strainers upside down in a new 50-mL conical tube followed by a rinse with 5-mL PBS per each strainer. To release the microvessels and capillaries from the strainer, the buffer was forced through the filter by pipetting up and down with a P1000 pipette. Vessels collected onto 100 μm and 20 μm strainers were collected in the same 50-mL conical tube and were centrifuged at 900g for 5 min at 4°C to pellet the vessels. The supernatant was carefully aspirated, and vascular pellets, designated as brain microvessels (BMV) were then processed for proteomics, immunofluorescence and RNA extraction. Vessel-depleted brain filtrates

were also collected to analyze protein expression in brain parenchyma.

RNA isolation

RNA was extracted from isolated BMVs by using RNeasy Plus Mini kit (Qiagen, Toronto, ON), while NucleoSpin RNA plus kit (Macherey–Nagel GmbH & Co. KG) was used for RNA isolation from all other tissues following manufacturer's protocols. Genomic DNA contamination was removed by Turbo DNA-Free Kit (Life Technologies/ThermoFisher Scientific, Nepean, ON). RNA quality was assessed using Agilent Bioanalyzer 2100 (Santa Clara, CA).

RNA-seq

RNA-Seq Libraries were generated using the TruSeq strand RNA kit (Illumina, San Diego, CA). The RNA-Seq libraries were quantified by Qbit and qPCR according to the Illumina Sequencing Library qPCR Quantification Guide and the quality of the libraries was evaluated on Agilent Bioanalyzer 2100 using the Agilent DNA-100 chip (Santa Clara, CA). The RNA-Seq library sequencing was performed using Illumina Next-Seq 500. FASTQ file format was processed by trimming the adaptor sequences, filtering low-quality reads (Phred Score ≤ 20) and eliminating short reads (length ≤ 20 bps) using software package FASTX-toolkit [http://hannonlab.cshl.edu/fastx_toolkit/]. STAR (v2.5.3a) [44] was used for the alignment of reads to the reference genome and to generate gene-level read counts. RSEM (version 1.3.3) [45] was used for alignment, to generate Transcripts per million (TPM) count. Mouse reference genome (version GRCm38.p6, M24), human reference genome (version GRCh38.p13, Genecode 33) and corresponding annotations were used as references for RNA-seq data alignment process. DESeq 2 [46] was used for data normalization and differentially expressed gene identification for each pair-wise comparison.

Public data sets and analysis

RNA-seq and microarray data in the public domains were obtained to compare/benchmark the data generated from this study for quality and comparability purposes. For RNA-seq data, raw data corresponding to normal lung and brain samples were obtained from the Sequence Read Archive [47] from the Genomics Data Commons [48]. GTEx data were processed using GDC reference files using GDC mRNA analysis pipeline (STAR two-pass) [44]. These data were combined with 12 samples analyzed at NRC and processed using DESeq 2 [46].

Automated Western blot analysis (Wes™)

Human and mouse BMVs were lysed in Cellytic MT buffer (Sigma) with 1 X Complete protease inhibitor (Roche) pellets on ice. The lysates were incubated on ice for 30 min, vortexed, then centrifuged at $21,000\times g$ for 10 min in a Sorvall Legend Micro 21R centrifuge. Protein concentrations were determined using the Quantipro BCA Assay Kit (Sigma). Wes was run using the 12–230kDa separation module (ProteinSimple), and the mouse or rabbit detection module (ProteinSimple Inc., San Jose, CA). Wes samples (protein at 0.8 mg/mL) were prepared by combining Master Mix to sample in a 1:4 ratio. Samples and Biotinylated Ladder were heated in a Accublock digital dry bath at 95 °C for 5 min. Samples were cooled to room temperature, vortexed to mix and centrifuged in a Mandel mini microfuge. Biotinylated ladder, samples, primary and secondary antibodies, and luminol were loaded on the plate and Wes was run using the standard protocol. Primary antibodies were rabbit anti-IGF1 receptor β (Cell Signaling, 3027S), mouse anti-transferrin receptor (Invitrogen, 13-6800) and rabbit anti-LRP1 (Abcam, ab925443). Primary antibodies were cross-reactive with human and mouse IGF1R, LRP1 and TfR proteins. Streptavidin-HRP was used to detect the ladder proteins. Data for each sample was first normalized to β -actin in the same lane. The level of the protein in mouse BMV was set as one fold. The fold-change of human protein was calculated relative to mouse protein (Mean \pm SD).

Immunofluorescence

Isolated brain microvessels in PBS (5 μ L) were deposited on Superfrost Plus slides (Fisher Scientific, Toronto, ON) and air-dried for 30 min. Samples were then fixed in Methanol (Fisher Scientific, Toronto, ON) for 15 min at room temperature and followed by incubation in 5% Normal Goat or Normal Donkey Serum (Jackson ImmunoResearch, West Grove, PA) in 0.2% Triton X-100 (Sigma, Oakville, ON) solution for 1 h at room temperature. The vessels were incubated with CD31 antibody 1:300 (BD Biosciences, San Jose, CA), Collagen IV antibody 1:300 (Millipore, Etobicoke, ON) or Griffonia Simplicifolia Lectin I (GSL-1) 1:500 (Vector Labs, Burlingame, CA). The primary antibodies for TfR, LRP-1 and IGF1R are the same as used above for Wes™ analyses. Secondary antibodies used were Goat anti-Rat and Donkey anti-Goat Alexa conjugated (Fisher Scientific, Toronto, ON) at 1:500 dilutions for 1 h at room temperature. Samples were mounted in Fluorescent Mounting Medium (Dako, Santa Clara, CA) containing 2 μ g/mL Hoechst (Fisher Scientific, Toronto,

ON). Images were acquired using Zeiss Axiovert 200 M microscope with 20 \times objective.

Tissue-Immunocytochemistry

Isolated brain vessels were air-dried for 15 min on slide warmer at 37 °C and fixed using commercially available Zinc 10 \times fixative (diluted to 1x with MQH₂O) for 90 min at RT. The slides were rinsed 3 times with PBS containing 0.05% tween-20 and blocked with Dako serum-free protein block containing 0.1% Triton-X 100 for 1 h at room temperature (RT). Endogenous peroxidase was quenched with 3% H₂O₂ in PBS for 15 min RT. The slides were rinsed 3 times with PBS containing 0.05% tween-20. IGF1R antibody (at 1:100 dilution; Cell Signaling 3027S lot13) was applied to the slides for 2 h RT (diluted in Dako antibody diluent containing 0.05% Triton-X 100). The slides were washed 3 times with PBS containing 0.05% tween-20 (at 2 min each). Secondary biotinylated goat anti-rabbit antibody was then applied to the slides for 45 min RT (1:250, diluted in Dako antibody diluent). The slides were washed 3 times with PBS containing 0.05% tween-20 (at 2 min each). RTU Horseradish peroxidase Avidin D was then applied for 30 min at RT. The slides were washed 3 times with PBS containing 0.05% tween-20 (at 2 min each). Color was developed 8 min with DAB substrate kit Vector labs SK4100. Slides were counterstained using hematoxylin, then dehydrated, cleared and cover slipped with xylene-based mounting media. The slides were visualized by Olympus IX81 inverted microscopy (Richmond Hill, ON). Images were acquired using Olympus IX81 inverted microscopy with 20 \times objective.

Nano LC-MS/MS analysis

Peptides from digested proteins prepared as described [10] were analyzed on a reversed-phase nanoAcquity UPLC (Waters, Milford, MA) coupled with a LTQ-XL mass spectrometer (ThermoFisher, Waltham, MA) with a nano-electrospray interface operated in positive ion mode. The analysis involved injection and loading of 0.6–1 μ g of mouse brain protein onto a 300 μ m I.D. \times 0.5 mm 3 μ m PepMaps® C18 trap (ThermoFisher) followed by eluting onto a 100 μ m I.D. \times 10 cm 1.7 μ m BEH130C18 nanoLC column (Waters). The mobile phase consisted of 0.1% (v/v) formic acid in water as buffer A and 0.1% (v/v) formic acid in acetonitrile as buffer B. The peptides were separated using a gradient ramping from 0.1 to 45% buffer B over 40 min, 45%–85% buffer B over 2 min, and then re-equilibrating from 85 to 0.1% buffer B over 10 min at a flow rate of 600 nL/min. The eluted peptides were ionized by electrospray ionization (ESI). Data were acquired on ions with mass/charge (m/z) values between 350 and 2000 followed by

three data-dependent MS/MS scans using collision-induced dissociation (CID) for fragmentation of the peptide ions.

Statistical analysis

The data from multiple groups were analyzed and compared using One-way ANOVA followed by Tukey's multiple comparisons test. Unpaired two-tailed student *t* test was used to compare data between two groups. $p < 0.05$ is considered statistical significance.

Results

Characterization of isolated brain microvessels (BMVs)

Mouse (Fig. 1a–e) and human (Fig. 1f–i) BMVs isolated using a modified separation protocols described [43] were characterized by immunofluorescence staining for the endothelial antigen CD31/PECAM-1, the basement membrane component collagen IV and the astrocyte (end-feet) marker glial fibrillary acidic protein (GFAP). The luminal surface of endothelial cells was visualized using lectin GSL-1 (Fig. 1b), which binds mouse endothelial glycocalyx. BMVs exhibited a strong immunoreactivity for CD31/PECAM-1 (Fig. 1a, c), continuous staining with the abluminal marker collagen IV, as well as a weak and 'spotty' immunoreactivity for GFAP (Fig. 1e, g). The majority of vessels in analyzed samples measured less than 20 μm in diameter.

The enrichment of cell-specific markers in BMVs in comparison to *vessel-depleted* brain parenchyma, was also analyzed using targeted nanoLC-MS/MS. A relative BMV enrichment of specified proteins was presented in Log₂ ratio in Fig. 2. *Endothelial cell markers* coagulation factor VIII-related antigen (F8), E-selectin (Sele), VE-cadherin (Cdh5) and Pecam1/CD31 showed 4 to eightfold enrichment in BMV preparations compared to vessel-depleted brain parenchyma; brain-endothelial cell-specific Slc2a1/glucose transporter (Glut1) showed over 60-fold enrichment in BMVs. *Pericyte markers*, platelet-derived growth factor receptor beta (Pdgfrb), desmin (Des), smooth muscle actin (Acta2), and CD13 (aminopeptidase N/Anpep), were also enriched in BMVs (2 to sixfold), whereas *astrocyte markers* glial fibrillary acidic protein (Gfap), protein S100-beta (S100 β), electrogenic sodium bicarbonate cotransporter 1 (Slc4a4), and aquaporin-4 (Aqp4) were 2 to fourfold enriched in brain parenchyma compared to BMVs. This data confirms that BMV isolation protocol used in this study yielded endothelial cell- and pericyte-enriched microvessels with significant depletion of astrocytes, although remnants of the astrocytic end-feet could still be detected by in situ immunofluorescence.

RNA-seq datasets: comparability and validation

Isolated mouse and human BMVs and organs were subjected to RNA-seq analyses; an enrichment of RMT receptors in BMVs was compared to peripheral organs and the whole brain (without vascular depletion).

When RNA-seq data generated in this study for human (total) brain and lung were compared with public RNA-seq data, a strong correlation (Pearson correlation coefficient of 0.96) (Additional file 1: Figure S1A, B) was observed. Comparison of biological replicates (brain total, lung total and brain vessels) analyzed in this study also showed high correlation (Pearson correlation coefficients ranging between 0.94 and 0.97, Additional file 1: Figure 1c–e). These analyses confirmed internal reproducibility and comparability of the RNA-seq data generated in this study with available 'benchmark' external datasets.

Further quality control of the dataset was performed by analyzing a relative enrichment of endothelial or BBB-specific gene transcripts in BMVs compared to (total) brain. Gene transcripts encoding *endothelial cell* genes Glut-1, VE-cadherin, E-selectin, CD31, tight-junction protein 1 (TJP1)/ZO1, occludin (OCLN), ABC transporter (ABCG2) and enzymes alkaline phosphatase (ALP) and γ -glutamyl transpeptidase (γ -GTP) were highly enriched in BMVs compared to the total brain in both mouse and human samples (Fig. 3a). Pericyte marker genes similarly were enriched in brain vessels relative to total brain tissues (Fig. 3b); while the transcript abundances of the *astrocyte*-specific glutamate transporters GLAST1 and SLC1A6 were higher in the brain than in the BMV (Fig. 3b).

The expression of RMT genes in isolated human BMVs, brain and lung

The expression levels of genes encoding RMT receptors in isolated human BMVs, total brain and lung tissues are listed in Table 1. The SLC2A1/GLUT-1 was the most abundant among the genes expressed in human BMVs (Table 1). The rank order of other RMT receptor transcript abundance in human BMVs was LRP1 > SLC3A2/CD98hc > CDC50A/TMEM30A > INSR > TFRC > LDLR > IGF1R > LEPR > LRP8 = IGF2R (Table 1; Fig. 4a). LRP1, SLC3A2/CD98hc and CDC50A were expressed at similar levels, and were significantly higher than all other RMT receptors studied (Fig. 4a).

INSR showed higher abundance (enrichment) in isolated human BMVs compared to either the brain or the lung (Table 1). SLC3A2/CD98hc, CDC50/TMEM30A and IGF1R were expressed at similar levels in brain vessels, brain and lung; whereas TFRC, LRP1, LDLR,

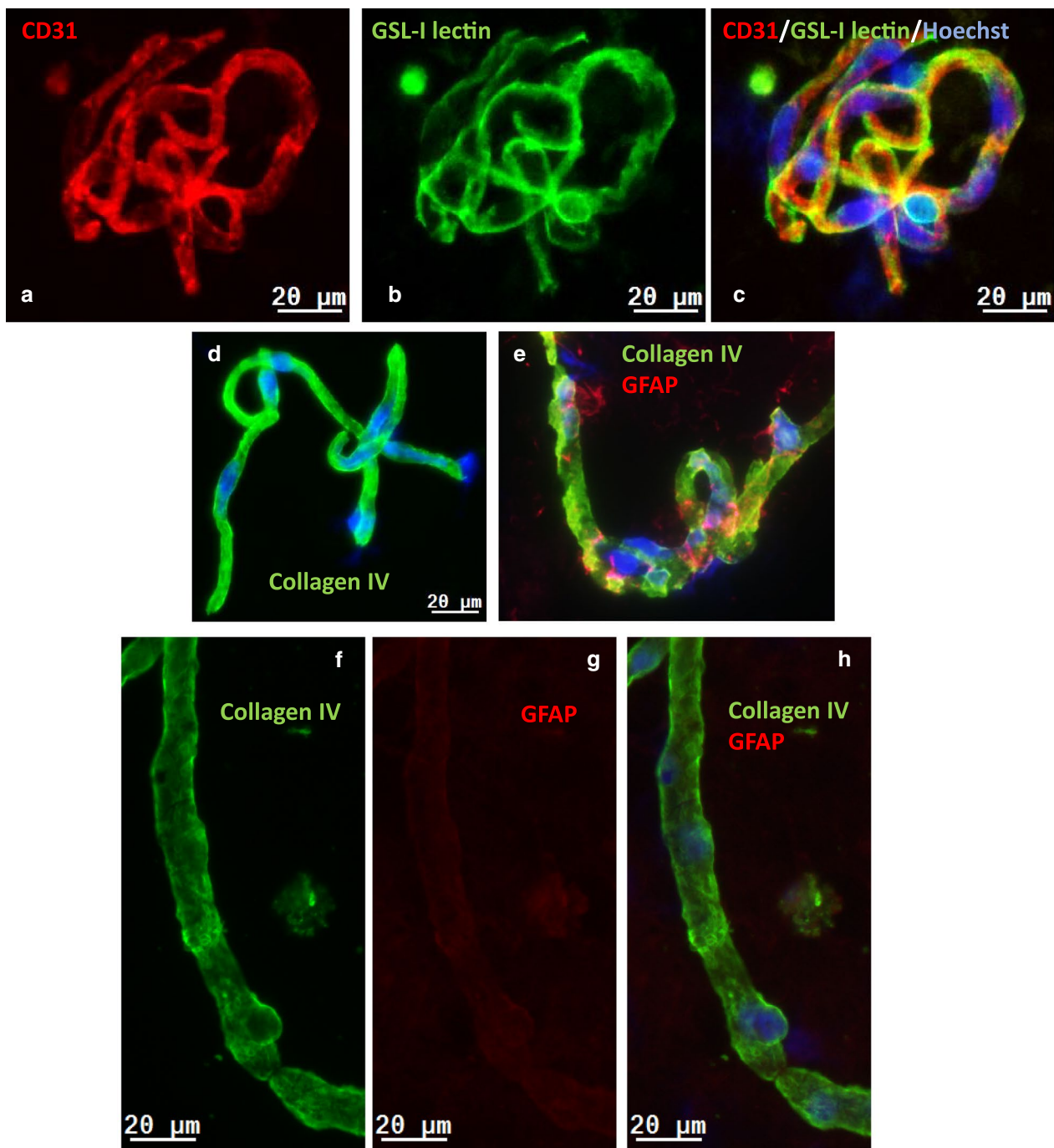
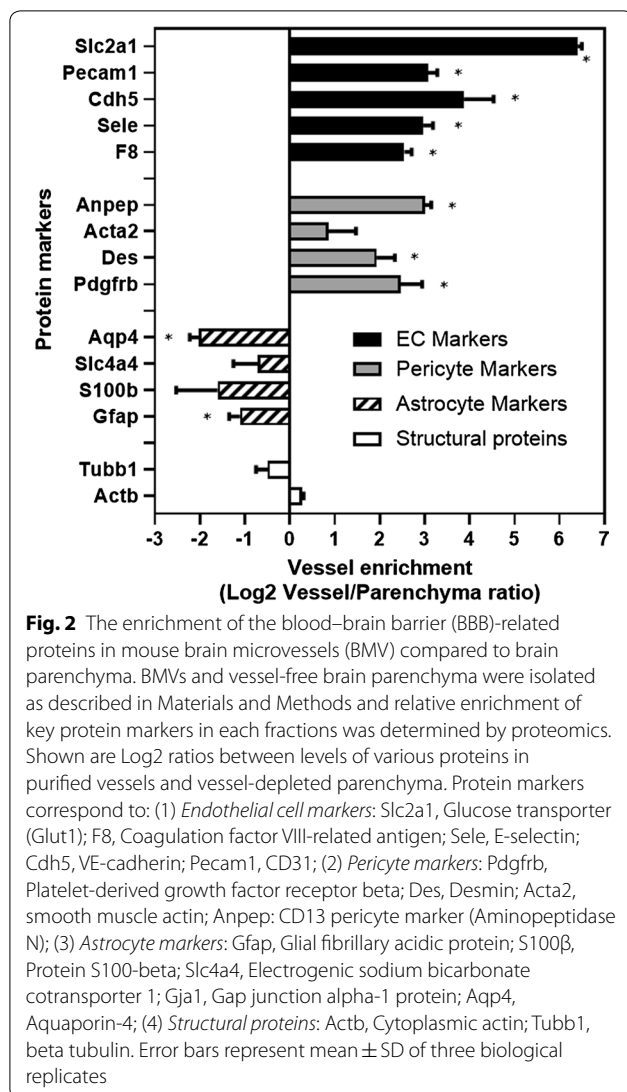


Fig. 1 Immunofluorescence analysis of isolated brain microvessels and capillaries (BMV) from the mouse (a–e) and human (f–i) brain. **a** CD31 immunofluorescence (red) in mouse BMV; **b** GSL-I lectin staining (green) in mouse BMV. **c** A composite image of CD31, GSL-I and Hoechst-stained nuclei (blue) of the same BMV. **d** Collagen IV immunofluorescence (green) in mouse BMV. **e** A composite image of collagen IV (green) and GFAP (red) immunofluorescence and Hoechst-stained nuclei (blue) in mouse BMV. **f** Collagen IV immunofluorescence of human BMV. **g** GFAP immunofluorescence of human BMV. **h** A composite image of of collagen IV (green) and GFAP (red) immunofluorescence and Hoechst-stained nuclei (blue) in human BMV. **i** Hoechst staining of nuclei in human BMV. The scale bar is 20 μm



IGF2R and LEPR were comparatively highly enriched in the lung (Table 1).

The expression of RMT genes in isolated mouse BMVs, lung microvessels, brain, liver and spleen

RNA-seq analyses were performed on isolated mouse BMVs, lung vessels, and whole tissue extracts of the brain, liver and spleen (Table 2; Fig. 4b). The gene showing the highest abundance and selectivity in isolated mouse BMVs was SLC2A1/GLUT1 (Table 2). Among other putative RMT receptors/transporters, the rank order in abundance in mouse BMVs was LRP1 > IGF1R = SLC3A2/CD98hc > CDC50A = LRP8 = TFRC = INSR > LDLR = IGF2R > LEPR (Table 2; Fig. 4b).

SLC2A1, IGF1R, INSR and LRP8 were distinctly enriched in mouse BMVs compared to the brain, lung vessels and peripheral tissues examined in this study

(Table 2). TFRC showed high transcript abundance in both BMVs and the spleen; whereas SLC3A2/CD98hc showed high transcript abundance in the spleen and lung vessels. CDC50A was enriched in the brain, liver and lung vessels (Table 2). IGF2R and LEPR showed relative enrichment in lung microvessels; while LDLR was highly expressed in liver, spleen and lung vessels (Table 2).

Cellular source of RMT receptor transcripts enriched in mouse and human BMVs

Comparisons of normalized RNA abundance of RMT receptors in human and mouse BMVs (from the current study) and available public datasets obtained from brain endothelial cells, astrocytes and neurons, as well as the whole brain and lung from corresponding species are shown in Additional file 1: Figure S2A, B. Data included in these analyses were obtained by single-cell sequencing of freshly isolated cells from the mouse brain vascular segments [49] and from the fetal and adult human cortex [49–51].

Comparative analyses suggested that the endothelial enrichment in SLC2A1, TfR, INSR, SLC3A2/CD98hc and LRP8 is largely responsible for the high abundance of these genes observed in the isolated mouse BMVs [50, 51]; observed LRP1 expression in mouse BMVs appears to originate from its abundance in pericytes and astrocytes; whereas observed expression levels of IGF1R, CDC50A and SLC2A1/Glut-1 may originate from either one or all three cell types forming the neurovascular unit (NVU). A recent publication by Kalucka et al. [52], which mapped single-cell transcriptome atlas of murine endothelial cells, identified IGF1R, TfR, LRP8 and SLC2A1 as highly enriched in BEC compared to endothelial cells from all other tissues; IGF1R transcript was threefold more abundant than TfR in BEC [52]. Human BMVs analyzed in this study appeared to have lower than expected expression of SLC2A1, TfR, LDLR, LRP8 and IGF1R compared to the endothelial expression of these genes derived from the single cell sequencing of the fetal and adult human cortex [49–51]. Similarly to what was observed with mouse BMVs, high LRP1 expression observed in human BMVs does not appear to originate from endothelial cells.

Species differences in the expression of RMT receptors in isolated human and mouse BMVs

The expression patterns of RMT receptors in BMVs and the whole brain of human and mouse were compared across species (Table 3). The abundance of receptor transcripts was compared across species using normalized transcripts per million (TPM) counts (Table 3).

The expression levels of SLC2A1, TFRC, LRP1, LRP8, IGF1R, IGF2R, CDC50A/TMEM30A and SLC3A2/CD98hc were all significantly higher in mouse BMVs

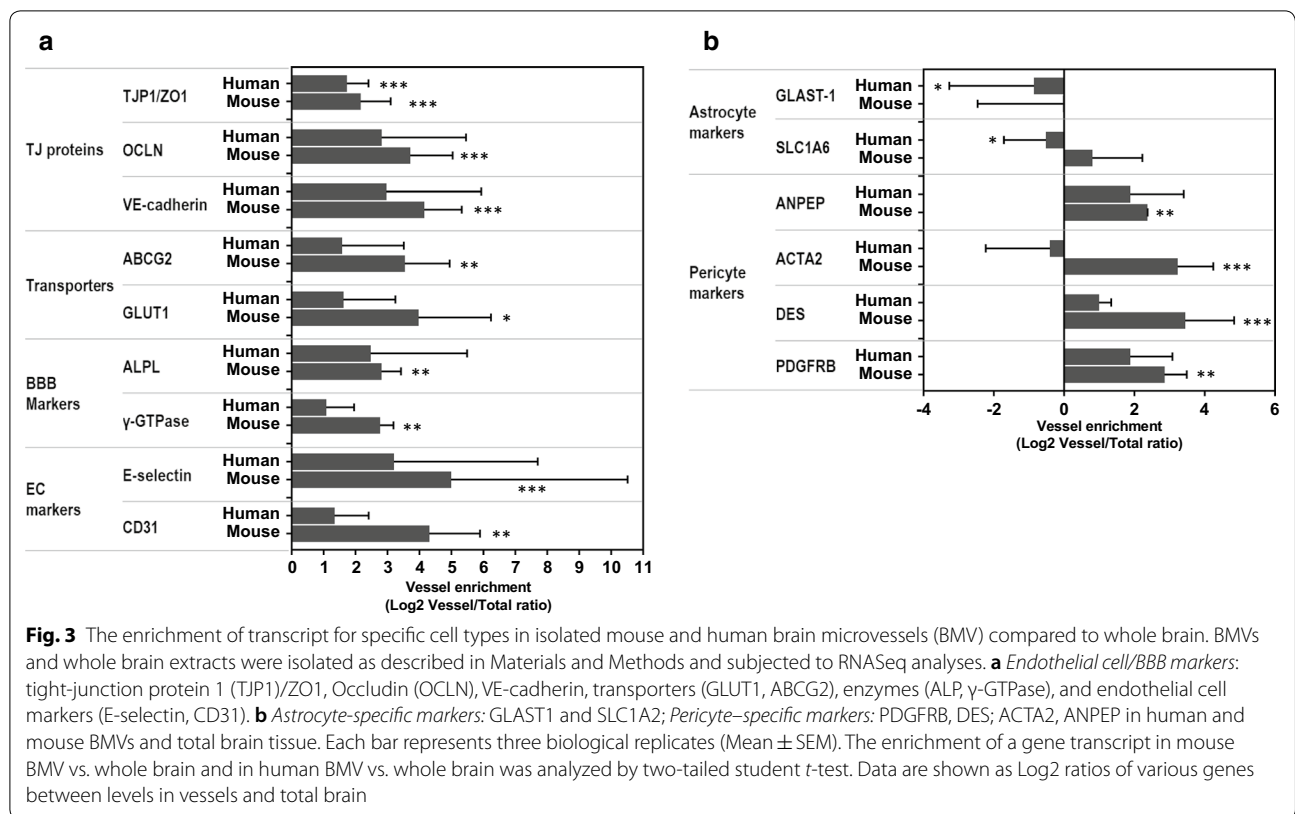


Table 1 Expression levels of genes encoding RMT receptors in isolated human brain microvessels (BMV), brain and lung (RNAseq normalized read counts; average ± SD)

Receptors/proteins	Human BMV	Human brain	Human lung
TFRC	1645.22 ± 249.68	1560.20 ± 520.04	7856.4 ± 6648.12
INSR	3010.84 ± 1158.90*	854.14 ± 81.00	1260.72 ± 106.44
IGF1R	1304.87 ± 746.61	905.46 ± 229.11	800.57 ± 198.75
IGF2R	602.08 ± 550.37	613.27 ± 194.15	4162.89 ± 2237.01*
LRP1	6896.83 ± 2520.15	5797.91 ± 1220.33	12,733.83 ± 4968.54
LDLR	1424.41 ± 2003.73*	294.13 ± 121.19	6952.95 ± 2791.13
LRP8 (ApoER2)	695.27 ± 650.56	734.55 ± 153.52	116.66 ± 69.72
CDC50A/TMEM30A	5578.82 ± 1174.14	7977.31 ± 2267.54	7621.38 ± 3189.82
SLC2A1/GLUT1	9579.89 ± 7741.88 [#]	3110.7 ± 1033.78	472.20 ± 217.86
SLC3A2/CD98hc	6527.14 ± 3983.38	4619.39 ± 509.35	5088.29 ± 425.63
LEPR	1131.17 ± 617.91*	1932.75 ± 612.91	3549.49 ± 132.05

Comparison of gene expression (transcript abundance) across isolated human BMVs, brain and lung was performed using One-way ANOVA, followed by Tukey's multiple comparisons test. Significant difference was indicated by (*). For simplicity, statistical significance was shown only for comparisons of BMV against other tissues (but not among other tissues)

*INSR expression in BMV was significantly (p < 0.05) higher compared to either brain or lung

*IGF2R expression in lung tissue was significantly (p < 0.05) higher compared to either brain vessels or brain

*LDLR expression in BMV was significantly higher (p < 0.001) compared to brain and significantly lower (p < 0.05) compared to lung

[#] SLC2A1/GLUT1: one sample out of 3 showed low transcript level, causing high SD. Therefore, despite overall high abundance, there was no significant difference compared to brain and lung. *LEPR expression in BMV was significantly lower compared to lung (p < 0.001)

(See figure on next page.)

Fig. 4 The abundance of RMT receptor and transporter gene transcripts in human (a) and mouse (b) brain microvessels (BMV). BMVs were isolated as described in Materials and Methods and subjected to RNASeq analyses. Data are shown as normalized read counts (Mean \pm SD from three biological replicates). Statistical analyses was performed using one-way ANOVA, followed by Tukey's multiple comparisons test and $p < 0.05$ was considered significant. For human BMV (a), the level of SLC2A1/GLUT1 is significantly higher than those of IGF2R, LRP8, and LEPR ($p < 0.05$). The level of SLC3A2/CD98hc is significantly higher than those of LDLR, LRP8, IGF1R, IGF2R and LEPR ($p < 0.05$). The level of LRP1 is significantly higher than those of TFRC, LDLR, IGF1R and LEPR ($p < 0.05$) and LRP8 and IGF2R ($p < 0.01$). For mouse BMV (b), the level of SLC2A1/GLUT1 is significantly higher than those of TFRC, INSR, IGF1R, IGF2R, LDLR, LRP8, CDC50A, and LEPR ($p < 0.0001$), and LRP1 ($p < 0.001$). The level of SLC3A2/CD98hc is significantly higher than those of TFRC and INSR ($p < 0.05$), LDLR, IGF2R and LEPR ($p < 0.0001$). The level of LRP1 is significantly higher than those of TFRC, INSR, IGF2R, LDLR, LRP8 and LEPR ($p < 0.0001$) and CDC50A ($p < 0.001$). The level of IGF1R is significantly higher than those of TFRC and INSR ($p < 0.01$), CDC50A ($p < 0.05$), IGF2R and LEPR ($p < 0.0001$). The level of TFRC is significantly higher than those of IGF2R ($p < 0.05$) and LEPR ($p < 0.01$). The level of LRP8 is significantly higher than those of IGF2R ($p < 0.05$) and LEPR ($p < 0.01$). The level of CDC50A is significantly higher than those of IGF2R and LEPR ($p < 0.01$)

compared to human BMVs (Table 3). The expression levels of LRP8, LDLR and LEPR were not significantly different in BMVs between two species (Table 3). LRP1, LRP8 and CDC50A/TMEM30A were more enriched in the mouse compared to human brain (Table 3).

The structural genes (GAPDH and S100B) were similarly expressed in mouse and human BMVs, and TUBB4A was expressed at similar levels in human and mouse BMVs and brains (Table 3).

IGF1R, LRP1 and TfR protein expression in human and mouse BMVs

Some of the above findings were validated at the protein expression level using the same BMV preparations that were analyzed by RNA-seq. Due to limited amount of BMV samples and based on the availability of species cross-reactive antibodies, three receptors were chosen against which antibodies/ligand were developed and tested as BBB-carriers in clinical (TfR, LRP-1) or advanced preclinical (IGF1R) studies. All three RMT receptors showed higher transcript abundance in mouse BMVs by RNA-seq. The protein expression of these RMT receptors was analyzed by Western blot (WesTM) and immunodetection.

TfR protein expression was higher in mouse BMVs compared to human BMVs by WesTM analyses (Fig. 5a, b; t -test $p < 0.05$) (normalized to β -actin). TfR was detected by immunofluorescence in both mouse (Fig. 5c–e) and human (Fig. 5f–h) BMVs.

The protein levels of LRP1 were also higher in mouse BMVs compared to human BMVs by WesTM analyses (Fig. 6a, b; t -test $p < 0.05$) (normalized to β -actin); strong immunofluorescence was detected in BMVs from both species around cell nuclei and borders and, occasionally, overlapping with collagen IV immunofluorescence (Fig. 6d, e, h, i).

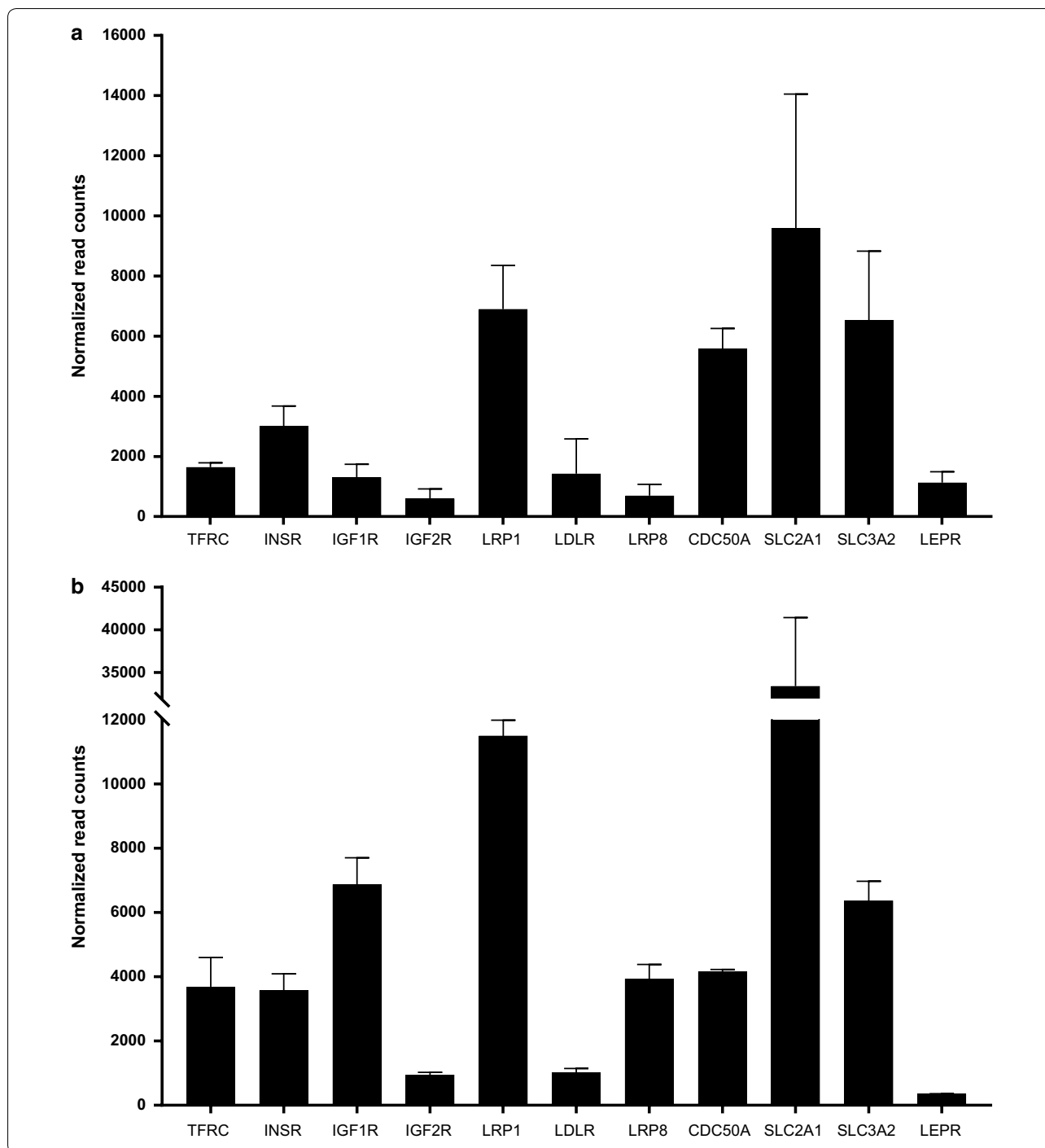
Western blot (WesTM) analysis demonstrated significantly lower expression of IGF1R in human compared to mouse BMVs (Fig. 7a, b; t -test $p < 0.0001$) (normalized

to β -actin). Immunofluorescence (Fig. 7c–g) and immunohistochemistry (Fig. 7h–i) analyses demonstrated a strong expression of IGF1R in both mouse (Fig. 7c, d) and human (Fig. 7e–i) BMVs, often observed as punctate, vesicular immunoreactivity in vessel walls. Immunostaining studies could not detect differences in IGF1R expression between mouse and human BMVs.

Discussion

Antibodies or peptide ligands against brain endothelial cell receptors that undergo RMT have been developed for brain delivery of therapeutic cargos. This strategy exploits a natural transport function of these receptors, which supply the brain with essential proteins (such as transferrin, insulin and insulin-like growth factors), peptides (such as leptin), essential amino acids, glucose or lipids. However, most of these receptors also play important functions and are expressed broadly or selectively in peripheral organs and tissues. In addition, their expression levels and distribution may vary in different species or pathologies, confounding translational development of BBB delivery carriers. The expression levels of genes encoding RMT receptors in different tissues and species have not been systemically investigated.

The selection of RMT receptors or other transporters for the development of BBB shuttles (carriers) should be guided by several criteria, including a) the selectivity of the expression in BEC compared to peripheral tissues and organs, to assure good systemic pharmacokinetics and to mitigate potential toxicity; b) low expression in brain parenchymal cells to avoid off-target distribution of the cargo, especially when cargo is an antibody against parenchymal target; c) abundance of the receptor in BEC to assure a sufficient transport capacity for a given application; d) similar patterns of expression in both BEC and other organs in experimental pre-clinical species and in humans to ensure translation of experimental findings to clinical application; e) the ability of ligands (natural or engineered) to the receptor to internalize into and to



transcytoses/release on the abluminal side of the brain endothelial cells.

To facilitate translational studies of BBB RMT carriers (shuttles) developed against various RMT receptors described in the literature (Additional file 1: Table S1), we have compared their abundance and enrichment in isolated mouse or human brain microvessels (BMVs) to

those in either the whole brain or peripheral tissues. The study revealed a significant species differences in selected RMT receptor abundance in different organs, as well as in BMVs.

The case study of TfR antibodies illustrates important translational hurdles in the pre-clinical to clinical development path of BBB carrier antibodies. TfR antibodies

Table 2 Expression levels of mouse genes encoding RMT receptors in isolated brain microvessels (BMV), whole brain, liver, spleen and lung vessels (RNAseq normalized read counts; average \pm SD)

Receptors/proteins	BMV	Brain	Liver	Spleen	Lung vessels
TFRC	3690.57 \pm 1577.32*	1366.54 \pm 198.69	824.73 \pm 70.64	3112.77 \pm 1853.22	358.11 \pm 79.98
INSR	3577.43 \pm 889.85*	956.02 \pm 215.79	1219.83 \pm 877.37	561.32 \pm 212.32	1475.28 \pm 84.75
IGF1R	6876.68 \pm 1430.93*	1102.77 \pm 297.56	38.19 \pm 27.33	386.79 \pm 70.17	1920.06 \pm 367.45
IGF2R	952.45 \pm 129.07	705.28 \pm 248.38	413.13 \pm 188.02	926.11 \pm 358.19	1531.46 \pm 133.94*
LRP1	11,506.40 \pm 833.68*	8489.28 \pm 1692.30	4448.88 \pm 920.24	3403.74 \pm 934.22	6397.87 \pm 829.14
LDLR	1015.42 \pm 223.35	584.67 \pm 170.78	2210.82 \pm 1160.86	850.94 \pm 230.47	1062.21 \pm 116.65
LRP8 (ApoER2)	3937.6 \pm 777.50*	1318.88 \pm 271.37	15.31 \pm 20.31	310.13 \pm 107.61	36.57 \pm 12.07
CDC50A/TMEM30A	4159.55 \pm 119.32*	8495.71 \pm 1376.15	13,191.59 \pm 2020.86	2457.55 \pm 424.88	3534.28 \pm 715.38
SLC2A1/GLUT1	33,418.54 \pm 13,876.59* [#]	2127.85 \pm 246.70	216.14 \pm 34.86	1164.86 \pm 192.17	478.96 \pm 48.42
SLC3A2/CD98hc	6369.22 \pm 1046.86*	2665.44 \pm 27.16	979.66 \pm 147.88	7792.42 \pm 1947.03	5596.12 \pm 929.74
LEPR/leptin receptor	356.37 \pm 14.03*	90.68 \pm 1.77	107.97 \pm 9.58	667.06 \pm 116.16	1917.86 \pm 469.42

Comparisons of gene expression (transcript abundance) across isolated mouse BMVs and peripheral tissues was performed using one-way ANOVA, followed by Tukey's multiple comparisons test. For simplicity, statistical significance was shown only for comparisons of BMVs against other tissues (but not among peripheral tissues)

*TFRC expression in BMV was significantly ($p < 0.05$) higher compared to lung vessels

*INSR expression in BMV was significantly higher ($p < 0.01$) compared to brain, liver, lung vessels or spleen

*IGF1R expression in BMV was significantly ($p < 0.0001$) higher compared to brain, liver, spleen or lung vessels

*IGF2R expression in lung vessels was significantly higher compared to brain tissue ($p < 0.01$) and liver ($p < 0.001$)

*LRP1 expression in BMV was significantly ($p < 0.01$) higher compared to liver, spleen, or lung vessels

*LRP8 expression in BMV was significantly ($p < 0.0001$) higher compared to brain, liver, spleen or lung vessels

*CDC50A/TMEM30A expression in BMV was significantly ($p < 0.01$) lower compared to brain or liver

*SLC2A1/GLUT1 expression in brain vessels was significantly ($p < 0.001$) higher compared to brain tissue, liver, spleen and lung vessels

[#] SLC2A1/GLUT1 expression was significantly ($p < 0.001$) higher in BMV compared to the expression of all other genes shown in Table 2

*SLC3A2/CD98hc expression in BMV was significantly higher ($p < 0.01$) compared to brain or liver

*LEPR expression in BMV was significantly ($p < 0.0001$) lower compared to lung vessels or spleen and significantly ($p < 0.001$) higher compared to brain or liver

with various characteristics have been developed for delivery of biotherapeutic cargos across the BBB, notably TfR/BACE1 bispecific antibody [7] and an anti-A β antibody fused to a single TfR-binding Fab fragment [37]. TfR is highly expressed in reticulocytes causing on-target toxicity of effector-function competent antibodies [38]; high-affinity TfR antibodies also exhibit poor pharmacokinetics due to peripheral target-mediated clearance [42, 53]. Due to lack of species cross-reactivity of TfR antibodies, the development of transgenic mouse expressing human TfR extracellular domain [7, 12, 13, 37], use of surrogate antibody or of transgenic mouse expressing human TfR [14, 15, 37] were necessary in pre-clinical studies. The translational PK-PD models developed based on these studies [54] did not take into account differences in TfR abundance between mouse and human. Comparative analyses of the TFRC expression performed in this study demonstrated a significantly higher abundance of TFRC in the mouse compared to human BMVs. In both human and mouse BMVs, TfR abundance was lower than those of SLC3A2/CD98hc and LRP1. Clinical trials with TfR antibodies as BBB carriers have been initiated by Roche (to deliver A β -antibody for

treatment of Alzheimer's disease) and by JCR Pharma (to deliver iduronate-2-sulfatase enzyme for treatment of Mucopolysaccharidosis II) [42]. These studies will provide further understanding of how differential TfR abundance in the brain vasculature, the brain and peripheral tissues between pre-clinical mouse species and humans may influence pharmacokinetics, toxicity and brain exposure of TfR antibody-containing biologics tested in the clinic.

Our study further found that: 1) INSR, IGF1R, LRP1 and LRP8 were enriched in the mouse BMVs compared to peripheral tissues; and INSR was enriched in human BMVs compared to total brain and lung; 2) SLC2A1/GLUT1, LRP-1, SLC3A2/CD98hc and CDC50A were the most abundant among receptor/transporters studied in human BMVs; whereas SLC2A1/GLUT1, LRP-1, SLC3A2/CD98hc and IGF1R were the most abundant in mouse BMVs; 3) mouse BMVs have significantly higher abundance of TfR, INSR, IGF1R, LRP-1, LRP8 and CDC50A compared to human BMVs.

The caveat of the current study is that RMT gene transcripts were analyzed in isolated BMVs which contain more than one cell type. A strong endothelial enrichment

Table 3 Expression levels of genes encoding RMT receptors in isolated human and mouse brain microvessels (BMV) and whole brain tissues [RNAseq normalized for transcript per million (TPM); Mean \pm SD]

Receptors/proteins	Human BMVs	Human brain	Mouse BMV	Mouse brain
TFRC	8.81 \pm 4.43	11.25 \pm 2.80	70.53 \pm 32.21*	20.85 \pm 4.41 [#]
INSR	5.44 \pm 3.70	4.75 \pm 0.49	33.09 \pm 8.63*	8.08 \pm 3.31
IGF1R	2.38 \pm 1.65	2.86 \pm 0.69	61.06 \pm 13.70*	7.36 \pm 2.33 [#]
IGF2R	3.09 \pm 3.42	3.88 \pm 2.06	9.88 \pm 1.40*	5.86 \pm 2.57
LRP1	21.18 \pm 16.53	28.80 \pm 6.61	179.85 \pm 15.66*	69.87 \pm 15.36 [#]
LDLR	14.04 \pm 19.25	5.19 \pm 1.55	21.21 \pm 5.00	9.67 \pm 3.66
LRP8 (ApoER2)	6.09 \pm 6.13	5.58 \pm 1.75	20.66 \pm 5.65	89.11 \pm 20.41 [#]
CDC50A/TMEM30A	28.62 \pm 16.30	68.42 \pm 15.01	98.36 \pm 1.58*	158.57 \pm 13.88 [#]
SLC2A1/GLUT1	86.20 \pm 88.50	41.64 \pm 12.54	1314.53 \pm 559.01*	64.62 \pm 1.08 [#]
SLC3A2/CD98hc	86.68 \pm 75.46	89.37 \pm 3.74	406.81 \pm 66.31*	138.96 \pm 14.72 [#]
LEPR/leptin receptor	2.25 \pm 1.96	1.19 \pm 0.32	1.35 \pm 1.35	2.10 \pm 0.71
GAPDH	1563.77 \pm 301.52	3924.81 \pm 295.78	1571.31 \pm 237.26	2824.45 \pm 442.70 ^{&}
S100B	520.09 \pm 180.37	1005.79 \pm 308.03	547.96 \pm 5.82	231.91 \pm 33.28 ^{&}
TUBB4A	328.93 \pm 126.15	363.04 \pm 92.13	357.16 \pm 110.37	552.25 \pm 194.57

Statistical comparison of gene expression (transcript abundance) between human and mouse BMVs and human and mouse brain was performed using two-tailed student *t*-test. Significant difference between human and mouse BMVs was indicated by (*) and significant difference between human and mouse brain is indicated by (#). *Receptor abundance is significantly higher (TFRC $p < 0.01$; INSR $p < 0.001$; IGF1R $p < 0.01$; IGF2R $p < 0.05$; LRP1 $p < 0.001$; LRP8 $p < 0.001$; CDC50A $p < 0.01$; SLC3A2 $p < 0.01$; SLC2A1 $p < 0.01$) in mouse compared to human BMVs

[#] Receptor expression is significantly higher (TFRC $p < 0.05$; IGF1R $p < 0.05$; LRP1 $p < 0.05$; LRP8 $p < 0.005$; CDC50A $p < 0.002$; SLC2A1 $p < 0.05$; SLC3A2 $p < 0.01$) in mouse compared to human brain

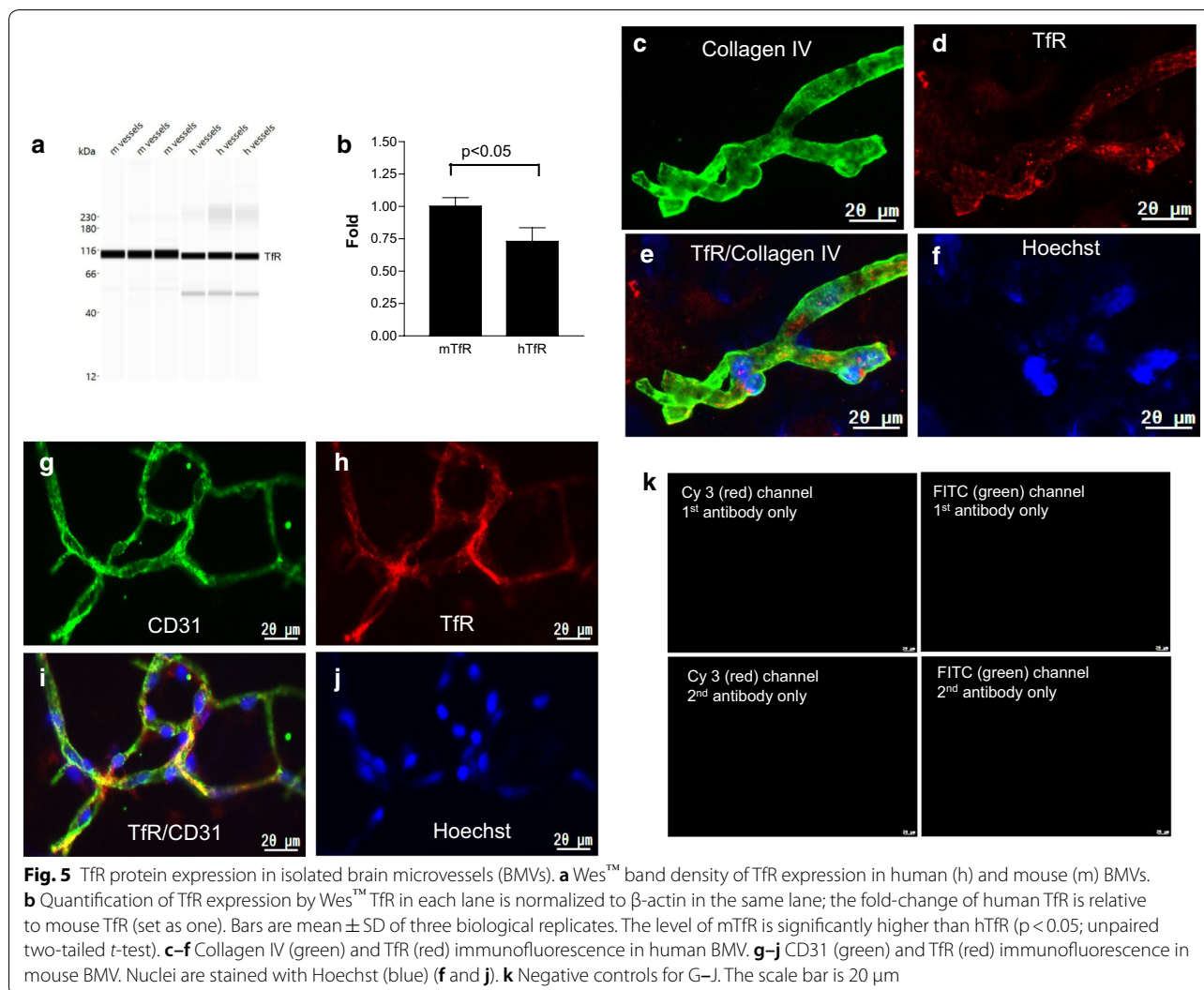
[&] Genes encoding structural proteins: S100B is significantly ($p < 0.001$) lower in mouse compared to human brain; GAPDH is significantly lower in mouse compared to human brain ($p < 0.05$)

in our BMV preparations has been confirmed by RNA-seq, targeted proteomics and immunofluorescence analyses; however, the presence of contaminating pericytes and astrocytic end-feet still confound the interpretation of the results. Therefore it is important to interpret results from this study in conjunction with the data obtained by other published studies that analyzed transcript profiles in brain cells or vascular segments using single-cell sequencing [20, 49, 52]. Human BMVs from this study showed comparatively lower expression of TfR, IGF1R, LRP8, LDLR and LEPR from that found in BEC obtained by the single-cell sequencing of human brain [20]. While transcript dilution as a result of the presence of multiple cell types, notably pericytes, in microvessel preparations compared to the purified cells, the other factors such as age of the donors, could also contribute to this observation. In contrast, RMT receptor expression in mouse BMVs was comparatively similar to that observed in BEC by the single-cell sequencing of mouse brain vessels [19], with the exception of the higher expression of LRP1 in isolated BMVs. Single-cell sequencing studies of human and mouse brain and brain vessels [19, 21] both found LRP-1 expression to be very low in BEC, in contrast to high expression in brain vascular smooth muscle cells, pericytes and fibroblast-like cells. A study in cultured bovine NVU cells showed eightfold higher expression of LRP-1 in pericytes compared to brain endothelial

cells [55]. This suggests that, despite being among the most abundant transcripts in isolated BMVs, LRP-1 expression originates from non-endothelial cells. This also brings into question its postulated role as BEC RMT receptor useful for therapeutic delivery across the BBB; it should be noted that antibodies raised against LRP1 failed to show facilitated BBB crossing [34].

Using proteomic survey, Zuchero et al. [34] found a very high abundance of basigin (BSG), followed by TfR and SLC3A2/CD98hc, whereas LRP1 was expressed at very low levels in freshly isolated endothelial cells from the mouse brain. RNA-seq data of mouse BMVs in this study ranked the abundance of SLC3A2/CD98hc higher than that of TfR, and similar to that of IGF1R. SLC3A2/CD98hc was also strongly expressed in the mouse spleen, consistent with the reported high expression levels in lymphocytes [56]. In contrast, SLC3A2/CD98hc expression was low in both human and mouse whole brain tissues.

Among the putative RMT receptors analyzed, SLC2A1 and IGF1R showed the highest selectivity of expression in mouse BMVs compared to all peripheral tissues, as well as the whole brain. IGF1R transcript levels were twofold more abundant than the TfR in mouse BMVs and were similar to that of the TfR in human BMVs. A recent single-cell transcriptomics study of endothelial cells in various mouse vascular beds [52], also found IGF1R highly



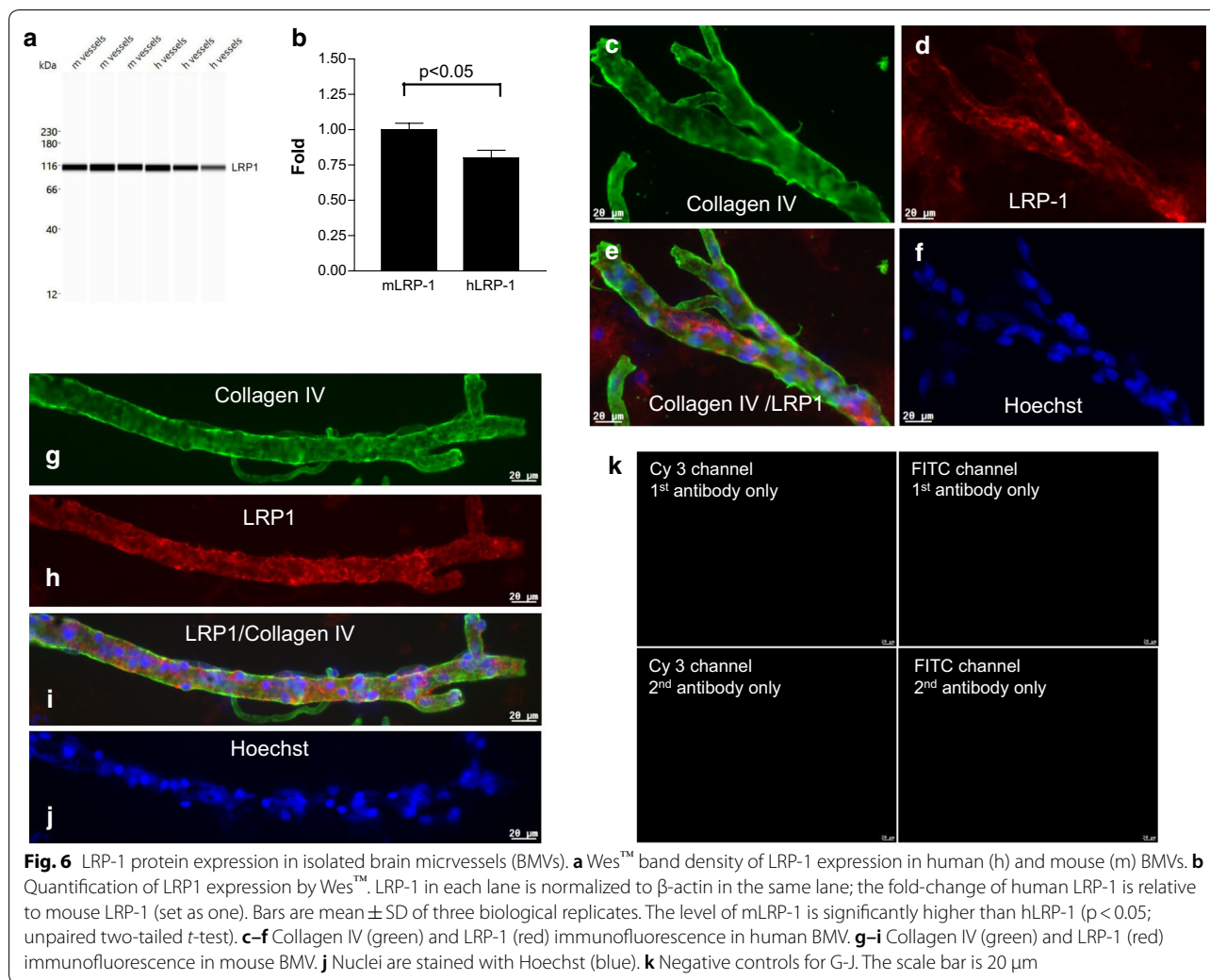
enriched in BEC and threefold more abundant than Tfr. In contrast, IGF2R exhibited low abundance in BMVs and high levels in lung tissues. This is consistent with the known developmental down-regulation of IGF2R in adult BBB, also accompanied by the lost ability of the receptor to facilitate transport of mannose 6-phosphate enriched lysosomal storage enzymes into the brain [57].

The additional caveat of transcriptomics studies is that the protein expression/function does not always correlate with the transcript abundance in given tissues. For example, a quantitative proteomics study of transporters and receptor in isolated human BMVs observed higher expression of Tfr (2.34 ± 0.76 fmol/ μ g protein) compared to either LRP-1 (1.51 ± 0.26 fmol/ μ g protein) or INSR (1.09 ± 0.21 fmol/ μ g protein) [58], whereas in this study the LRP-1 transcript abundance in human BMVs was the highest among studied putative RMT receptors; albeit likely due to its enrichment in pericytes. Our

within-study comparisons between the transcript abundance and the protein expression by Wes analysis for Tfr, LRP-1 and IGF1R showed similar trends of lower expression of IGF1R and Tfr in human compared to mouse BMVs; whereas no difference was found for LRP1. A species cross-reactive antibodies used in these studies make true quantification of expression levels difficult; for example immunodetection studies with the same antibodies did not detect appreciable expression differences between human and mouse BMVs, likely because antigen retrieval and antibody reactivity to antigenic epitopes in two methods are very different.

Conclusion

This study provides a molecular transcriptomics map of key RMT receptors in mouse and human brain microvessels, brain and peripheral tissues, important to

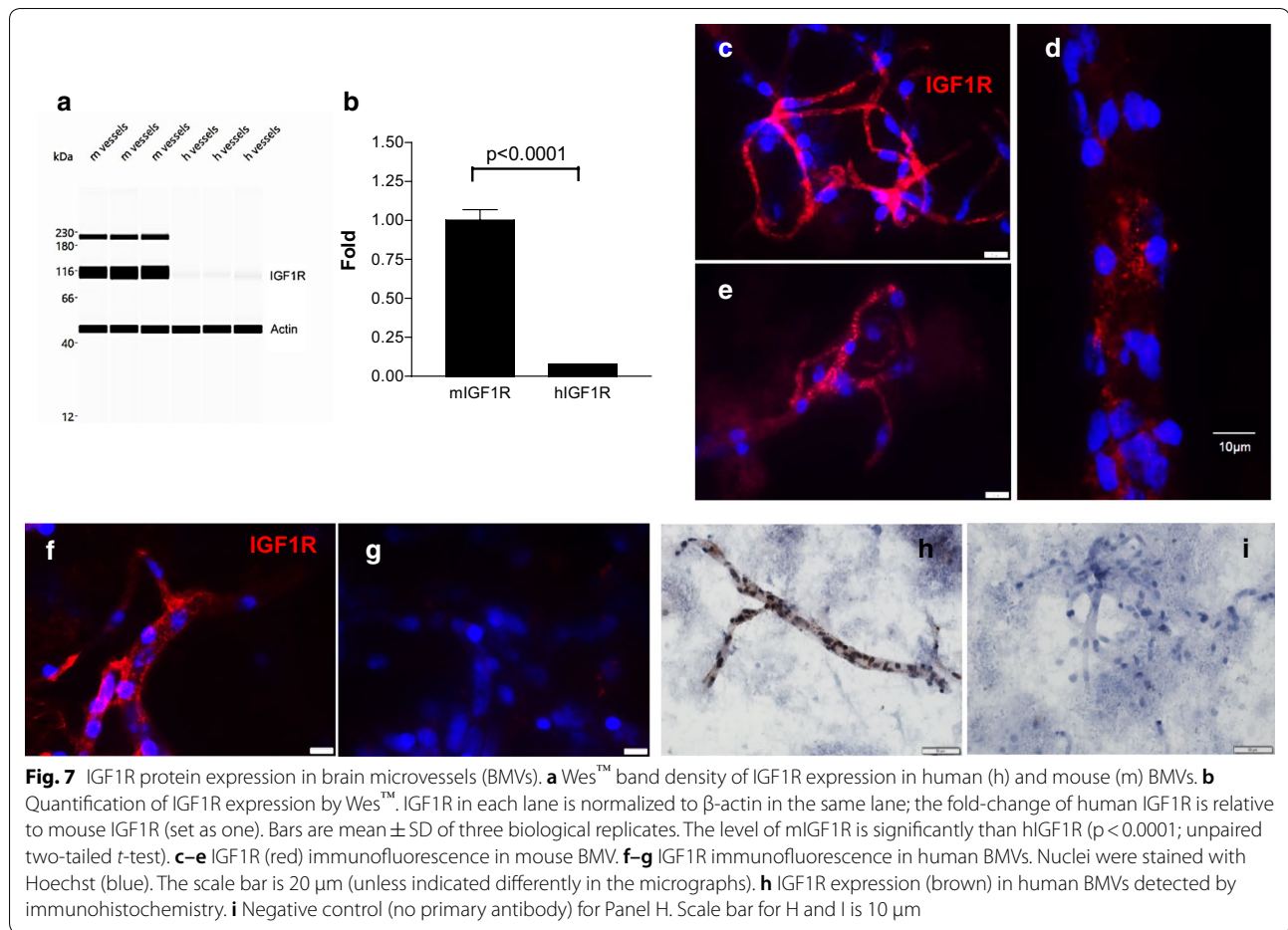


translational studies of biodistribution, efficacy and safety of antibodies developed against these receptors.

RMT receptor genes in brain microvessels, brain parenchyma and peripheral organs from human and mouse were analyzed by RNA-seq and validated by Western blot and in situ immunodetection. SLC2A1, IGF1R, INSR and LRP8 were highly enriched in mouse BMVs compared to peripheral tissues; additionally SLC2A1 and IGF1R showed high abundance in mouse BMVs. Antibodies against IGF1R have been shown to internalize into brain endothelial cells; while antibodies against both these targets (SLC2A1 and IGF1R) showed enhanced total brain levels in mice compared to control antibodies (although in the absence of vessel depletion for SLC2A1 antibodies). Among evaluated receptors, IGF1R and SLC2A1 appear to satisfy most of the criteria for promising targets to develop trans-BBB delivery ligands; however, it should be understood that SLC2A1 is a carrier-mediated transporter unlikely to undergo a

typical RMT. In addition to desired characteristics of the target receptor, development and optimization of an optimized ligand/antibody against these targets is essential for achieving success in improved delivery of biotherapeutics across the BBB.

Cross-species differences in the expression of RMT in BMVs, brain and peripheral tissues is an important consideration in translational studies to advance BBB carriers developed against these receptors into clinical trials. This study suggests that the mouse BBB expresses many of targeted RMT receptors at higher levels than the human BBB. Since the mouse is the most widely used pre-clinical model for discovery and evaluation of investigational compounds, including brain delivery 'shuttles', translational studies and PK-PD modeling to estimate dosing in humans need to account for species differences in RMT receptor abundance in BEC and different organs.



Supplementary information

Supplementary information accompanies this paper at <https://doi.org/10.1186/s12987-020-00209-0>.

Additional file 1. Additional figures and tables.

Abbreviations

BBB: Blood–brain barrier; BEC: Brain endothelial cells; BMV: Brain microvessels; GFAP: Glial fibrillary acidic protein; GLUT-1/SLC2A1: Glucose transporter-1; γ-GTP: γ-Glutamyl transpeptidase; INSR: Insulin receptor; IGF1R: Insulin-like growth factor-1 receptor; IGF2R: Insulin-like growth factor-2 receptor; LDLR: Low-density lipoprotein receptor; LRP-1: LDLR-related protein 1; LRP8: LDLR-related protein 8; LEPR: Leptin receptor; RMT: Receptor-mediated transcytosis; CMT: Carrier-mediated transcytosis; TMEM30A/CDC50A: Transmembrane protein 30A; TFRC: Transferrin receptor (gene); Tfr: Transferrin receptor (protein).

Acknowledgements

Not applicable.

Authors' contributions

WZ analyzed data, designed some of the experiments, drafted figures, wrote and revised the manuscript; QYL designed the RNA-seq experiments, performed some data analysis, drafted part of the manuscript; ASH designed some of the experiments (proteomics), performed some data analysis, drafted some figures and figure legends; SL isolated RNA, prepared RNA-seq libraries and performed RNA sequencing; ZL normalized the RNAseq datasets; FF performed some data analysis, drafted some figures and wrote parts of

the manuscript; Ewa B isolated brain vessels, dissected animal tissues and performed immunohistochemistry on brain vessels; CED isolated brain vessels and dissected animal tissues; DL performed preliminary RNA-seq data analyses; ATS performed MS proteomics experiments; Eric B dissected mice and collected tissues; CS performed Wes analyses; MH performed immunohistochemistry; JKS designed the immunohistochemistry/immunofluorescence experiments; DBS conceived the experiments and contributed to writing of the manuscript. All authors read and approved the final manuscript.

Funding

The research was supported by funding from the National Research Council Canada (NRC) and conducted at the NRC Human Health Therapeutics Research Centre

Availability of data and materials

The RNA-seq data is presented in Tables 1, 2 and 3, and the dataset used and/or analyzed in this study is available from the corresponding author on reasonable request.

Consent for publication

The manuscript does not contain any individual person's data in any form.

Competing interests

The authors declare no conflict of interest.

Author details

¹ Human Health Therapeutics Research Centre, National Research Council of Canada, 1200 Montreal Road, M54, Ottawa, ON K1A0R6, Canada. ² Scientific

Data Mining/Digital Technology Research Centre, National Research Council of Canada, Ottawa, Canada.

Received: 2 March 2020 Accepted: 13 July 2020

Published online: 22 July 2020

References

- Abbott NJ, Patabendige AA, Dolman DE, Yusof SR, Begley DJ. Structure and function of the blood–brain barrier. *Neurobiol Dis.* 2010;37(1):13–25.
- Lajoie JM, Shusta EV. Targeting receptor-mediated transport for delivery of biologics across the blood–brain barrier. *Annu Rev Pharmacol Toxicol.* 2015;55:613–31.
- Fishman JB, Rubin JB, Handrahan JV, Connor JR, Fine RE. Receptor-mediated transcytosis of transferrin across the blood–brain barrier. *J Neurosci Res.* 1987;18(2):299–304.
- Duffy KR, Pardridge WM. Blood–brain barrier transcytosis of insulin in developing rabbits. *Brain Res.* 1987;420(1):32–8.
- Pardridge WM, Buciak JL, Friden PM. Selective transport of an anti-transferrin receptor antibody through the blood–brain barrier in vivo. *J Pharmacol Exp Ther.* 1991;259(1):66–70.
- Friden PM, Walus LR, Musso GF, Taylor MA, Malfroy B, Starzyk RM. Anti-transferrin receptor antibody and antibody-drug conjugates cross the blood–brain barrier. *Proc Natl Acad Sci U S A.* 1991;88(11):4771–5.
- Yu YJ, Zhang Y, Kenrick M, Hoyte K, Luk W, Lu Y, Atwal J, Elliott JM, Prabhu S, Watts RJ, Dennis MS. Boosting brain uptake of a therapeutic antibody by reducing its affinity for a transcytosis target. *Sci Translational Med.* 2011;3:84ra44.
- Pardridge WM. Delivery of biologics across the blood–brain barrier with molecular trojan horse technology. *BioDrugs.* 2017;31(6):503–19.
- Bien-Ly N, Yu YJ, Bumbaca D, et al. Transferrin receptor (TfR) trafficking determines brain uptake of TfR antibody affinity variants. *J Exp Med.* 2014;211(2):233–44.
- Haqqani AS, Delaney CE, Brunette E, Baumann E, Farrington GK, Sisk W, Eldredge J, Ding W, Tremblay TL, Stanimirovic DB. Endosomal trafficking regulates receptor-mediated transcytosis of antibodies across the blood brain barrier. *J Cereb Blood Flow Metab.* 2018;38(4):727–40.
- Villaseñor R, Lampe J, Schwaninger M, Collin L. Intracellular transport and regulation of transcytosis across the blood–brain barrier. *Cell Mol Life Sci.* 2019;76(6):1081–92.
- Kariolis MS, Wells RC, Getz JA, Kwan W, Mahon CS, Tong R, Kim DJ, Srivastava A, Bedard C, Henne KR, Giese T, Assimon VA, Chen X, Zhang Y, Solanoy H, Jenkins K, et al. Brain delivery of therapeutic proteins using an Fc fragment blood–brain barrier transport vehicle in mice and monkeys. *Sci Transl Med.* 2020;12(545):eaay1359. <https://doi.org/10.1126/scitranslmed.aay1359>.
- Ullman JC, Arguuello A, Getz JA, Bhalla A, Mahon CS, Wang J, Giese T, Bedard C, Kim DJ, Blumenfeld JR, Liang N, Ravi R, Nugent AA, Davis SS, Ha C, Duque J, Tran HL, Wells RC, Lianoglou S, Daryani VM, Kwan W, Solanoy H, Nguyen H, Earr T, Dugas JC, Tuck MD, Harvey JL, Reyzer ML, Caprioli RM, Hall S, Poda S, Sanchez PE, Dennis MS, Gunasekaran K, Srivastava AS, Sandmann T, Henne KR, Thorne RG, Paolo GD, Astarita G, Diaz D, Silverman AP, Watts RJ, Sweeney ZK, Kariolis MS, Henry AG. Brain delivery and activity of a lysosomal enzyme using a blood–brain barrier transport vehicle in mice. *Sci Transl Med.* 2020;12(545):eaay1163. <https://doi.org/10.1126/scitranslmed.aay1163>.
- Boado RJ, Pardridge WM. Brain and organ uptake in the rhesus monkey in vivo of recombinant iduronidase compared to an insulin receptor antibody-iduronidase fusion protein. *Mol Pharm.* 2017;14(4):1271–7.
- Boado R. Platform technology for treatment of brain disorders with blood–brain barrier penetrating IgG-fusion proteins: preclinical and clinical updates. The CHI's 5th Annual Blood–Brain Barrier Meeting, World Pharma Week, June 19–20, 2019 (Boston).
- Pardridge WM, Boado RJ, Giugliani R, Schmidt M. Plasma pharmacokinetics of valanafusp alpha, a human insulin receptor antibody-iduronidase fusion protein, in patients with mucopolysaccharidosis type I. *BioDrugs.* 2018;32(2):169–76.
- Uchida Y, Zhang Z, Tachikawa M, Terasaki T. Quantitative targeted absolute proteomics of rat blood–cerebrospinal fluid barrier transporters: comparison with a human specimen. *J Neurochem.* 2015;134(6):1104–15.
- Ito K, Uchida Y, Ohtsuki S, Aizawa S, Kawakami H, Katsukura Y, Kamiie J, Terasaki T. Quantitative membrane protein expression at the blood–brain barrier of adult and younger cynomolgus monkeys. *J Pharm Sci.* 2011;100(9):3939–50.
- Zhang Y, Chen K, Sloan SA, Bennett ML, Scholze AR, O'Keefe S, Phatnani HP, Guarnieri P, Caneda C, Ruderisch N, Deng S, Liddelow SA, Zhang C, Daneman R, Maniatis T, Barres BA, Wu JQ. An RNA-sequencing transcriptome and splicing database of glia, neurons, and vascular cells of the cerebral cortex. *J Neurosci.* 2014;34:11929–47.
- Darmanis S, Sloan SA, Zhang Y, Enge M, Caneda C, Shuer LM, Hayden Gephart MG, Barres BA, Quake SR. A survey of human brain transcriptome diversity at the single cell level. *Proc Natl Acad Sci U S A.* 2015;112(23):7285–90.
- Vanlandewijck M, He L, Mäe MA, Andrae J, Ando K, Del Gaudio F, Nahar K, Lebouvier T, Laviña B, Gouveia L, Sun Y, Raschperger E, Räsänen M, Zarb Y, Mochizuki N, Keller A, Lendahl U, Betsholtz C. Author Correction: A molecular atlas of cell types and zonation in the brain vasculature. *Nature.* 2018;560(7716):E3. (2018; 554: 475–480).
- He L, Vanlandewijck M, Mäe MA, Andrae J, Ando K, Del Gaudio F, Nahar K, Lebouvier T, Laviña B, Gouveia L, Sun Y, Raschperger E, Segerstolpe Å, Liu J, Gustafsson S, Räsänen M, Zarb Y, Mochizuki N, Keller A, Lendahl U, Betsholtz C. Single-cell RNA sequencing of mouse brain and lung vascular and vessel-associated cell types. *Sci Data.* 2018;5:180160.
- Stanimirovic D, Kemmerich K, Haqqani AS, Sulea T, Arbab-Ghahroudi M, Massie B, Gilbert R. Insulin-like growth factor 1 receptor-specific antibodies and uses thereof. WO2015131256A1. 2015.
- Ribecco-Lutkiewicz M, Sodja C, Haukenfrers J, Haqqani AS, Ly D, Zachar P, Baumann E, Ball M, Huang J, Rukhlova M, Martina M, Liu Q, Stanimirovic D, Jezierski A, Bani-Yaghoob M. A novel human induced pluripotent stem cell blood–brain barrier model: applicability to study antibody-triggered receptor-mediated transcytosis. *Sci Rep.* 2018;8(1):1873.
- Castellano JM, Deane R, Gottesdiener AJ, Verghese PB, Stewart FR, West T, Paoletti AC, Kasper TR, DeMattos RB, Zlokovic BV, Holtzman DM. Low-density lipoprotein receptor overexpression enhances the rate of brain-to-blood A β clearance in a mouse model of β -amyloidosis. *Proc Natl Acad Sci U S A.* 2012;109(38):15502–7.
- Demeule M, Régina A, Ché C, Poirier J, Nguyen T, Gabathuler R, Castaigne JP, Béliveau R. Identification and design of peptides as a new drug delivery system for the brain. *J Pharmacol Exp Ther.* 2008;324(3):1064–72.
- Demeule M, Currie JC, Bertrand Y, Ché C, Nguyen T, Régina A, Gabathuler R, Castaigne JP, Béliveau R. Involvement of the low-density lipoprotein receptor-related protein in the transcytosis of the brain delivery vector angiopep-2. *J Neurochem.* 2008;106:1534–44.
- Molino Y, David M, Varini K, Jabès F, Gaudin N, Fortoul A, Bakloul K, Masse M, Bernard A, Drobecq L, Lécorché P, Tamsamani J, Jacquot G, Khrestchatsky M. Use of LDL receptor-targeting peptide vectors for in vitro and in vivo cargo transport across the blood–brain barrier. *FASEB J.* 2017;31(5):1807–27.
- Masliah E, Spencer B. Applications of ApoB LDLR-binding domain approach for the development of CNS-penetrating peptides for Alzheimer's disease. *Methods Mol Biol.* 2015;1324:331–7.
- Jacquot G, Lécorché P, Malcor J-D, Laurencin M, Smirnova M, Varini K, Malicet C, Gassiot F, Abouzid K, Faucon A, David M, Gaudin N, Masse M, Ferracci G, Dive V, Cisternino S, Khrestchatsky M. Optimization and in vivo validation of peptide vectors targeting the LDL receptor. *Mol Pharm.* 2016;13:4094–105.
- Coleman JA, Molday RS. Critical role of the beta-subunit CDC50A in the stable expression, assembly, subcellular localization, and lipid transport activity of the P4-ATPase ATP8A2. *J Biol Chem.* 2011;286:17205–16.
- Muruganandam A, Tanha J, Narang S, Stanimirovic D. Selection of phage-displayed llama single-domain antibodies that transigrate across human blood–brain barrier endothelium. *FASEB J.* 2002;16:240–2.
- Anraku Y, Kuwahara H, Fukusato Y, Mizoguchi A, Ishii T, Nitta K, Matsumoto Y, Toh K, Miyata K, Uchida S, Nishina K, Osada K, Itaka K, Nishiyama N, Mizusawa H, Yamasoba T, Yokota T, Kataoka K. Glycaemic control boosts glucosylated nanocarrier crossing the BBB into the brain. *Nat Commun.* 2017;8(1):1001.
- Zuchero Y, Chen X, Bien-Ly N, Bumbaca D, Tong RK, Gao X, Zhang S, Hoyte K, Luk W, Huntley MA, Phu L, Tan C, Kallop D, Weimer RM, Lu Y, Kirkpatrick DS, Ernst JA, Chih B, Dennis MS, Watts RJ. Discovery of novel blood–brain

- barrier targets to enhance brain uptake of therapeutic antibodies. *Neuron*. 2016;89:70–82.
35. Liu Y, Li J-F, Shao K, Huang R-Q, Ye L-Y, Lou J-N, Jiang C. A leptin derived 30-amino-acid peptide modified pegylated poly-L-lysine dendrigraft for brain targeted gene delivery. *Biomaterials*. 2010;31(19):5246–57.
 36. Yu YJ, Atwal JK, Zhang Y, Tong RK, Wildsmith KR, Tan C, Bien-Ly N, Hersom M, Maloney JA, Meilandt WJ, Bumbaca D, Gadkar K, Hoyte K, Luk W, Lu Y, Ernst JA, Scearce-Levie K, Couch JA, Dennis MS, Watts RJ. Therapeutic bispecific antibodies cross the blood–brain barrier in nonhuman primates. *Sci Transl Med*. 2014;6(261):261ra154.
 37. Niewoehner J, Bohrmann B, Collin L, Ulrich E, Sade H, Maier P, Rueger P, Stracke JO, Lau W, Tissot AC, Loetscher H, Ghosh A, Freskgård PO. Increased brain penetration and potency of a therapeutic antibody using a monovalent molecular shuttle. *Neuron*. 2014;81:49–60.
 38. Couch J, Yu YJ, Zhang Y, Tarrant JM, Fuji RN, Meilandt WJ, Solano H, Tong RK, Hoyte K, Luk W, Lu Y, Gadkar K, Prabhu S, Ordonia BA, Nguyen Q, Lin Y, Lin Z, Balazs M, Scearce-Levie K, Ernst JA, Dennis MS, Watts RJ. Addressing safety liabilities of TFR bispecific antibodies that cross the blood–brain barrier. *Sci. Transl. Med*. 2013;5:183ra57.
 39. Wang L, Prasad B, Salphati L, Chu X, Gupta A, Hop CE, Evers R, Unadkat JD. Interspecies variability in expression of hepatobiliary transporters across human, dog, monkey, and rat as determined by quantitative proteomics. *Drug Metab Dispos*. 2015;43(3):367–74.
 40. Angiochem Inc. ANG1005 in breast cancer patients with recurrent brain metastases. *ClinicalTrials.gov* (<https://clinicaltrials.gov/ct2/show/NCT02048059>).
 41. ArmaGen Inc: <http://armagen.com/our-focus/hurler-syndrome/>.
 42. Okuyama T, Eto Y, Sakai N, Minami K, Yamamoto T, Sonoda H, Yamaoka M, Tachibana K, Hirato T, Sato Y. Iduronate-2-sulfatase with anti-human transferrin receptor antibody for neuropathic mucopolysaccharidosis ii: a phase 1/2 trial. *Mol Ther*. 2019;27:456–64.
 43. Webster CI, Caram-Salas N, Haqqani AS, Thom G, Brown L, Rennie K, Yogi A, Costain W, Brunette E, Stanimirovic DB. Brain penetration, target engagement, and disposition of the blood–brain barrier-crossing bispecific antibody antagonist of metabotropic glutamate receptor type 1. *FASEB J*. 2016;30:1927–40.
 44. Dobin A, Davis CA, Schlesinger F, Drenkow J, Zaleski C, Jha S, Batut P, Chaisson M, Gingeras TR. STAR: ultrafast universal RNA-seq aligner. *Bioinformatics*. 2013;29:15–21.
 45. Li B, Dewey CN. RSEM: accurate transcript quantification from RNA-Seq data with or without a reference genome. *BMC Bioinformatics*. 2011;12:323.
 46. Love MI, Huber W, Anders S. Moderated estimation of fold change and dispersion for RNA-seq data with DESeq2. *Genome Biol*. 2014;15:550.
 47. Leinonen R, Sugawara H, Shumway M. International nucleotide sequence database collaboration. The sequence read archive. *Nucleic Acids Res*. 2011;39(1):19–21.
 48. Grossman RL, Heath A, Murphy M, Patterson M, Wells W. A case for data commons: toward data science as a service. *Comput Sci Eng*. 2016;18(5):10–20.
 49. Zheng GX, Terry JM, Belgrader P, Ryvkin P, Bent ZW, Wilson R, Ziraldo SB, Wheeler TD, McDermott GP, Zhu J, Gregory MT, Shuga J, Montesclaros L, Underwood JG, Masquelier DA, Nishimura SY, Schnall-Levin M, Wyatt PW, Hindson CM, Bharadwaj R, Wong A, Ness KD, Beppu LW, Deeg HJ, McFarland C, Loeb KR, Valente WJ, Ericson NG, Stevens EA, Radich JP, Mikkelsen TS, Hindson BJ, Bielas JH. Massively parallel digital transcriptional profiling of single cells. *Nature Communications*. 2017;8:14049.
 50. Ulrich E, Lasic SE, Molnos J, Wells I, Freskgard PO. Transcriptional profiling of human brain endothelial cells reveals key properties crucial for predictive in vitro blood–brain barrier models. *PLoS ONE*. 2012;7(5):e38149.
 51. Huntley MA, Bien-Ly N, Daneman R, Watts RJ. Dissecting gene expression at the blood–brain barrier. *Front Neurosci*. 2014;8:355.
 52. Kalucka J, de Rooij LPMH, Goveia J, Rohlenova K, Dumas SJ, Meta E, Concinha NV, Taverna F, Teuwen LA, Veys K, García-Caballero M, Khan S, Geldhof V, Sokol L, Chen R, Treps L, Borri M, de Zeeuw P, Dubois C, Karakach TK, Falkenberg KD, Parys M, Yin X, Vinckier S, Du Y, Fenton RA, Schoonjans L, Dewerchin M, Eelen G, Thienpont B, Lin L, Bolund L, Li X, Luo Y, Carmeliet P. Single-Cell Transcriptome atlas of murine endothelial cells. *Cell*. 2020;180(4):764. <https://doi.org/10.1016/j.cell.2020.01.015>.
 53. Partridge WM, Boado RJ, Patrick DJ, Ka-Wai Hui E, Lu JZ. Blood–brain barrier transport, plasma pharmacokinetics, and neuropathology following chronic treatment of the rhesus monkey with a brain penetrating humanized monoclonal antibody against the human transferrin receptor. *Mol Pharm*. 2018;15(11):5207–16.
 54. Gadkar K, Yadav DB, Zuchero JY, Couch JA, Kanodia J, Kenrick MK, Atwal JK, Dennis MS, Prabhu S, Watts RJ, Joseph SB, Ramanujan S. Mathematical PKPD and safety model of bispecific TFR/BACE1 antibodies for the optimization of antibody uptake in brain. *Eur J Pharm Biopharm*. 2016;101:53–61. <https://doi.org/10.1016/j.ejpb.2016.01.009>.
 55. Candela P, Saint-Pol J, Kuntz M, Boucau MC, Lamartiniere Y, Gosselet F, Fenart L. In vitro discrimination of the role of LRP1 at the BBB cellular level: focus on brain capillary endothelial cells and brain pericytes. *Brain Res*. 2015;1594:15–26.
 56. Cantor JM, Ginsberg MH. CD98 at the crossroads of adaptive immunity and cancer. *J Cell Sci*. 2012;125(6):1373–82.
 57. Urayama A, Grubb JH, Sly WS, Banks WA. Developmentally regulated mannose 6-phosphate receptor-mediated transport of a lysosomal enzyme across the blood–brain barrier. *Proc Natl Acad Sci USA*. 2004;101(34):12658–63. <https://doi.org/10.1073/pnas.0405042101>.
 58. Uchida Y, Ohtsuki S, Katsukura Y, Ikeda C, Suzuki T, Kamiie J, Terasaki T. Quantitative targeted absolute proteomics of human blood–brain barrier transporters and receptors. *J Neurochem*. 2011;117(2):333–45.

Publisher's Note

Springer Nature remains neutral with regard to jurisdictional claims in published maps and institutional affiliations.

Ready to submit your research? Choose BMC and benefit from:

- fast, convenient online submission
- thorough peer review by experienced researchers in your field
- rapid publication on acceptance
- support for research data, including large and complex data types
- gold Open Access which fosters wider collaboration and increased citations
- maximum visibility for your research: over 100M website views per year

At BMC, research is always in progress.

Learn more biomedcentral.com/submissions

